Deep UV generation and fs pulses characterization using strontium tetraborate

Aleksandrovsky, A., Vyunishev, A., Zaitsev, A., Ikonnikov, A., Pospelov, G., et al.

A. S. Aleksandrovsky, A. M. Vyunishev, A. I. Zaitsev, A. A. Ikonnikov, G. I. Pospelov, V. V. Slabko, A. A. Zhokhova, "Deep UV generation and fs pulses characterization using strontium tetraborate," Proc. SPIE 8071, Nonlinear Optics and Applications V, 80710K (18 May 2011); doi: 10.1117/12.886189

SPIE.

Event: SPIE Optics + Optoelectronics, 2011, Prague, Czech Republic

Deep UV generation and fs pulses characterization using strontium tetraborate

A.S. Aleksandrovsky*[ab], A.M. Vyunishev[ab], A.I. Zaitsev[ab], A.A. Ikonnikov[b],
G.I. Pospelov[b], V.V. Slabko[b], A.A. Zhokhova[b]
[a]Kirensky Institute of Physics, Akademgorodok 50/38, 660036, Krasnoyarsk, Russian Federation
[b]Siberian Federal University, Svobodniy 79, 660041, Krasnoyarsk, Russian Federation

ABSTRACT

The properties of NPC structures in strontium tetraborate are analyzed. Different types of NPC structures are revealed that possess different nonlinear properties, and their spectral dependences of frequency conversion efficiency are calculated and compared. Experimental study of these structures is reported for the process of doubling of the second harmonic of fs Ti:S laser. Tuning of generated radiation is obtained in the range 187.5 - 232.5 nm, with extreme insensitivity to the angular orientation of NPC. Behavior of tuning curve along investigated fundamental wave range is similar in all studied samples, but efficiency obtained depends on the type of structure. Conversion efficiency and spectral quality of generated radiation is experimentally shown to grow better when using NPC with improved structure. Prospects of VUV converter on a single NPC are discussed. NPCs of SBO are demonstrated to be useful for autocorrelation diagnostics both in random QPM geometry and in the geometry of nonlinear diffraction from virtual beam.

Keywords: nonlinear photonic crystal, strontium tetraborate, second harmonic generation, random quasi phase matching, ultrafast diagnostics.

1. INTRODUCTION

All-solid-state nonlinear optical techniques involving deep ultraviolet (DUV) and vacuum ultraviolet (VUV) radiation experience limitations due to increased crystalline absorption and dispersion in the vicinity of short-wavelength edge of transparency window in most known efficient nonlinear media. Increase in dispersion imposes the most severe restrictions in case when angular phase matching is used for enhancement of nonlinear process efficiency. In this sense, strontium tetraborate (SBO) nonlinear crystal is attractive from the point of view of VUV nonlinear optical generation due to its large bandgap. According to electronic structure calculations[1], indirect band gap of 9.71 eV (127 nm) and direct band gap of 11.18 eV (110 nm) are expected for pure SBO. These calculations are supported by experimental data[2] showing that SBO fundamental absorption edge lies at the shortest wavelength among all nonlinear crystals, namely, in the vicinity of 125 nm. Another advantage of SBO is the largest nonlinear coefficients among all crystals transparent below 270 nm. The drawback of SBO is the absence of angular phase matching. No data on ferroelectricity are available for this crystal; hence, the common techniques for production of quasi phase matching structures are not suitable for SBO.

The only way to employ the possibilities offered by SBO is provided by another unique feature of its crystal structure, namely, the existence of self-organized oppositely poled domains[3]. As far as we know, this property, while being common for ferroelectrics, was not observed in any other non-ferroelectric crystal except for SBO. These domains are highly randomized, and for any selected wavelength only partial quasi phase matching of nonlinearly generated radiation along the structure takes place. This leads to broadening of phase matching spectral dependencies accompanied with decrease of generated power with respect to perfect QPM structure. Since the refractive indices inside the structures can be considered to be homogeneous while the second order susceptibility is modulated, these domain structures must be classified to be a nonlinear photonic crystal (NPC)[4]. Random NPC are capable of phase matching the nonlinear conversion of broadband radiation, generally speaking, in any direction inside the crystal. Two limiting cases exist, namely, random quasi-phase-matching (RQPM) and nonlinear diffraction. Nonlinear diffraction is rarely used for efficient conversion in the practice of nonlinear optics, however, we have shown that it can be rather efficient even in

*aleksandrovsky@kirensky.ru; phone 7 391 249-4613; fax 7 391 243-8923

Nonlinear Optics and Applications V, edited by Mario Bertolotti, Proc. of SPIE Vol. 8071
80710K · © 2011 SPIE · CCC code: 0277-786X/11/$18 · doi: 10.1117/12.886189

case of highly randomized NPC SBO[5,6]. RQPM[7], from the point of view of conversion efficiency, takes the intermediate position between non-phase-matched case in a monodomain sample and quasi-phase-matched case in periodically poled nonlinear crystal (PPNC)[8]. The generated power in a single domain sample oscillates along the propagation direction with the period equal to double coherence length (in absence of phase matching), while in QPM case it grows according to square law with the domain number. In random NPC the generated power experiences irregular behavior but for the interaction lengths much larger than randomization length the average linear growth of generated power will be observed[7]. Decrease in efficiency of conversion in this case is the price for the tunability in a wide spectral range. Another feature of RQPM is the preservation of conversion efficiency if the fundamental wavelength and propagation direction are increased in accordance with each other[9]. This effect can be interpreted as so-called rotational red shift of the NPC band structure. The position and the width of individual subbands in the band structure depend on the domain geometry in the NPC, and it is interesting to examine its variation in different NPC samples.
There are two possible areas of applications for SBO, namely generation of DUV and VUV and diagnostics of ultrashort pulses generated using other techniques. In the present communication we report the results of comparative experimental study of the cascaded fourth harmonic generation of femtosecond pulses from Ti: Sapphire oscillator using RQPM in several different samples of NPC of SBO. Secondly, we report RQPM autocorrelation measurements using NPC SBO.

2. DOMAIN STRUCTURES IN SBO

SBO belongs to orthorhombic symmetry class *mm2*. Common notation for space symmetry group used in the following is $Pnm2_1$, the crystallographic axis *c* being the polar axis. Nonzero nonlinear coefficients are d_{caa}, d_{cbb}, d_{ccc}, d_{aac}, and d_{bbc}. Domain structures were found in as-grown crystals[3] obtained via Czochralski growth with single-domain seed crystals at temperature about 1000° C. Domains have the form of sheets with domain walls perpendicular to the *a* crystallographic axis. Similarly oriented domains are known in potassium titanyl phosphate (KTP) that belongs to the same symmetry class *mm2*. However, domains in KTP are formed in the course of phase transition from paraelectric into ferroelectric phase at 934° C, well below KTP melting point. Investigation of SBO crystals via DTA showed no any phase transitions between the room temperature and the melting point. This means that domain formation process in SBO differs from that in KTP. From general considerations, the former must be due to the instability of crystal structure at the surface between growing crystal and the melt, which may lead to spontaneous crystal structure reversal of a part of crystal. In case when newly formed structure enables better stability, the growing crystal will contain domain structure with the domains of random thickness determined by the degree of initial instability and by the randomness of spontaneous domain reversal. If crystal growth area is homogeneous in space and time, once formed sufficiently stable configuration of domains will be sustained till the end of growth process and will be perfectly uniform along *b* and *c* axes. In case when stability of the structure is not enough, deviations in domain thickness will appear due to subsequent partial reversal of crystal structure within existing domain structure. The same result can be observed in case of varying growth conditions, due to variation of stability requirements. In the latter cases domain structure is expected to have non-uniform thickness sequence along *b* and *c* axes.

The distribution of domain thickness in NPC is of great importance for the spectral dependence of a nonlinear optical process. An ideal case is when average domain thickness is equal to the coherence length for a process of interest, and randomization extent fits the spectral bandwidth of input radiation. For collinear nonlinear optical processes involving DUV or VUV radiation, the coherence length typically diminishes, due to increase of dispersion. Similar decrease is expected for the non-collinear processes. Required average domain thickness for collinear QPM L_C and for nonlinear diffraction[10] d_{ND} can be calculated using formulas

$$L_C = \frac{\pi}{\Delta k(\lambda)}, d_{ND} = \frac{\lambda}{4}\left(n_{p2}^2(\lambda/2) - n_{p1}^2(\lambda)\right) \qquad (1),$$

where $\Delta k(\lambda)$ is the wavevector mismatch, $n_{p2}^2(\lambda/2)$ and $n_{p1}^2(\lambda)$ are refractive indices at corresponding wavelengths with account for the polarization. Behavior of these parameters for frequency doubling using d_{ccc} nonlinear coefficient of SBO are presented in Fig.1. For instance, doubling of 400 nm radiation in NPC SBO requires average domains thickness of order of 0.9 μm, while doubling of 260 nm would require average domain thickness 130 nm. Tunable conversion to the wavelength range 200 to 130 nm, therefore, requires wide spectrum of domain thickness from 900 to 130 nm. Average domain thickness for nonlinear diffraction in the same spectral region ranges from 160 to 46 nm. It should be noted that if domains of required thickness were absent in a chosen NPC sample, it would contribute both to higher-order

RQPM and nonlinear diffraction, but the efficiency of nonlinear conversion will be smaller than in case of first order phase matching. From the point of view of reciprocal superlattice vectors (RSV), the thickness of domain walls can be of interest for the evaluating conversion to the VUV, since finite domain thickness means that larger RSV values necessary to compensate for larger wave detuning possess smaller amplitudes.

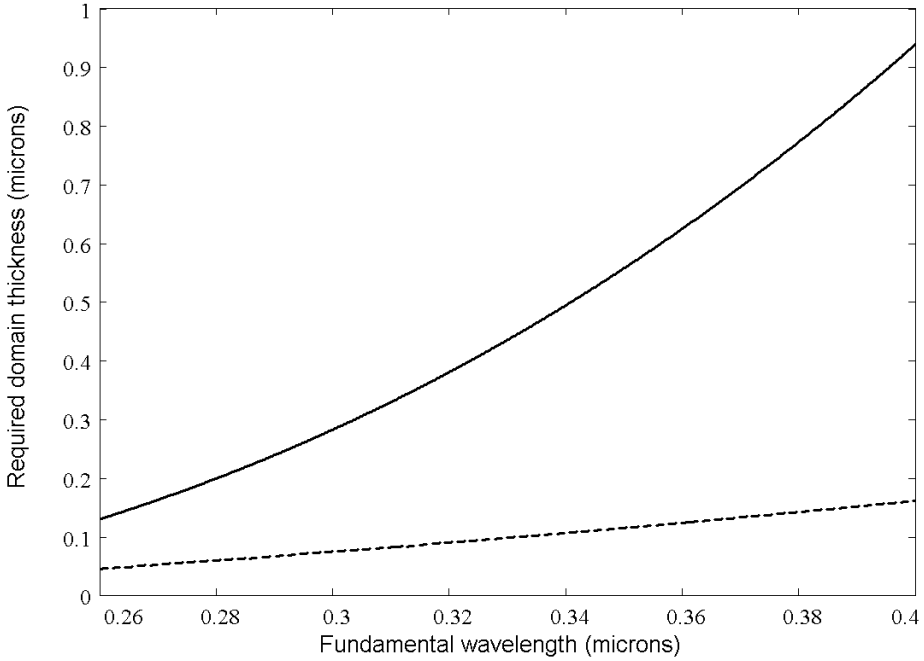

Figure 1. Dependence of required average domain thickness on the fundamental wavelength for frequency doubling in SBO using d_{ccc} nonlinear coefficient. Solid line corresponds to collinear RQPM, dashed line is for nonlinear diffraction.

From the point of view of domain reversal model described above, the lower and upper limits of domain thickness distribution is determined by the stability against splitting of, correspondingly, small spontaneously inverted domain and large non-splitted domain.

The images of several typical domain structures in SBO obtained during separate growth processes are presented in Fig.2. The visualization of domains is done via chemical etching of the facets perpendicular to polar axis. Images are obtained with the help of Carl Zeiss optical microscope, and despite the limitations imposed optical microscopy, detailed examination of images allows to identify domains of different orientations and to measure the thickness down to 0.5 μm. Smaller domains could be suggestively detected but the measurement of their thickness was less accurate. NPC samples obtained in separate growth processes are further referred as Samples 2, 4, 7 and 8 (the number are our internal notation, with no physical sense). The growth procedure for all these samples is identical within the accuracy of controlling instrumentation being used, however, resulting structures considerably differ. The Sample 2 contains domain structure with overall thickness 2 mm. The dimensions of domain structure in the *b* and *c* axes directions are about 1 cm. However, domain structure in *a* axis direction demonstrates morphological nonuniformity. Images a) and b) in Fig.2 present two different parts of the Sample 2. Structure in Fig. 2a contains the domain sequence with thickness of individual domains mainly from 0.5 to 2 μm, with comparatively small randomness. Thickness of domains with different orientation of the polar axis is approximately equal. Another part of the same sample contains thicker domains with dominant polarity and much more narrow domains with opposite polarity, and the degree of randomization is much higher. The latter is illustrated by the domain density plot for the whole domain structure in the Sample 2 (Fig. 2d). The spread of Sample 2 domain thickness is up to 180 μm, and the mean domain thickness is 8 μm. Image in Fig2c presents the part of the Sample 7 domain structure. This sample contained 1 mm thick quasi-homogeneous domain structure that is featured by thick domains of dominant polarity (upper limit of thickness is approximately 10 μm and mean domain thickness is 1 μm) and by thin domains of opposite polarity. This structure is somehow similar to that in Fig.2b, but the characteristic scale is much lower, and thickness distribution is narrower, as can be seen in the density plot (Fig. 2e). Samples 4 and 8 have the structure that is in general similar to that of the Sample 7.

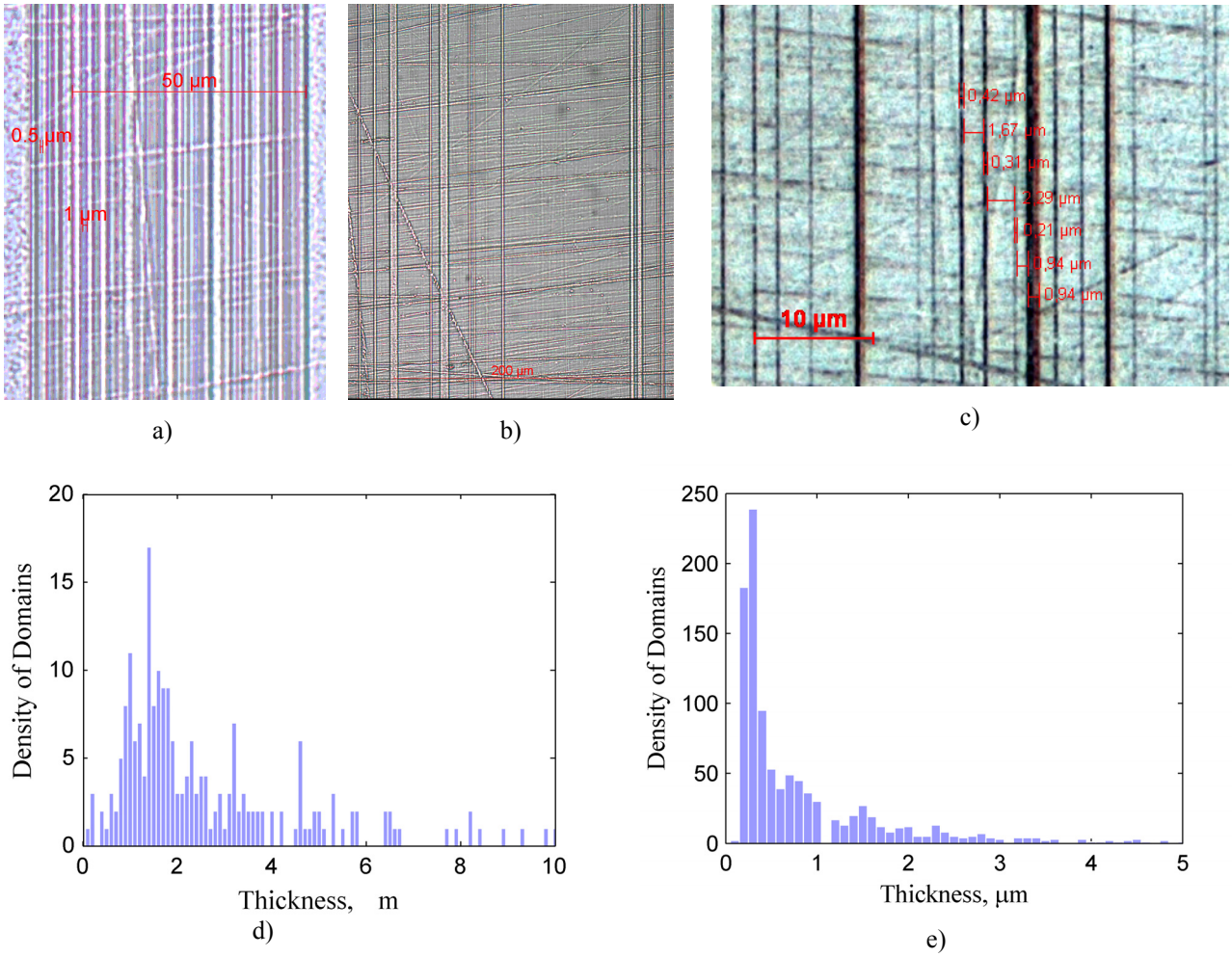

Figure 2. Examples of domain structures in SBO viewed from the polar axis *c* (a,b,c). Parts of density plots for Sample2 (d) and Sample 7 (e).

3. SPECTRAL PROPERTIES OF NPC SBO

As discussed in[8], the dependence of power generated in highly randomized NPC of SBO is featured by a large number of relatively narrow peaks occupying broad spectral range of fundamental wavelengths from near IR to UV. The simplest plane wave model for $\omega_1 + \omega_2 \rightarrow \omega_3$ conversion of monochromatic radiation in NPC that allows estimating spectral properties of a certain domain structure leads to the following expression for generated radiation field strength

$$E_3 = \sum_{n=1}^{N} \left\{ \frac{\omega_3^2 \chi_n^{(2)}}{k_3(\theta_{\text{int}})\Delta k(\theta_{\text{int}})} E_1 E_2 \cdot \left[\exp\left(i\Delta k(\theta_{\text{int}}) \frac{d_n}{\cos(\theta_{\text{int}})} \right) - 1 \right] \cdot \exp\left(i\Delta k(\theta_{\text{int}}) \sum_{r=n+1}^{N} \frac{d_r}{\cos(\theta_{\text{int}})} \right) \right\} \qquad (2),$$

where d_n is the thickness of nth domain, $\chi_n^{(2)} = (-1)^n \left| \chi^{(2)} \right|$ accounts for the opposite sign of nonlinear susceptibility in neighboring domains, N is the full number of domains, θ_{int} is internal angle of plane wave propagation, $\Delta k(\theta_{\text{int}})$ is the wave vector mismatch with account for anisotropy of refraction index. Fig.3a presents spectral dependence for second harmonic generated in a structure Fig.2a (solid line) in comparison with the same dependence for regular structure of the same thickness optimized for doubling 355 nm radiation (dashes, divided by 10). Fig.2b presents the same dependences for the full structure of the Sample 2 containing 262 domains.

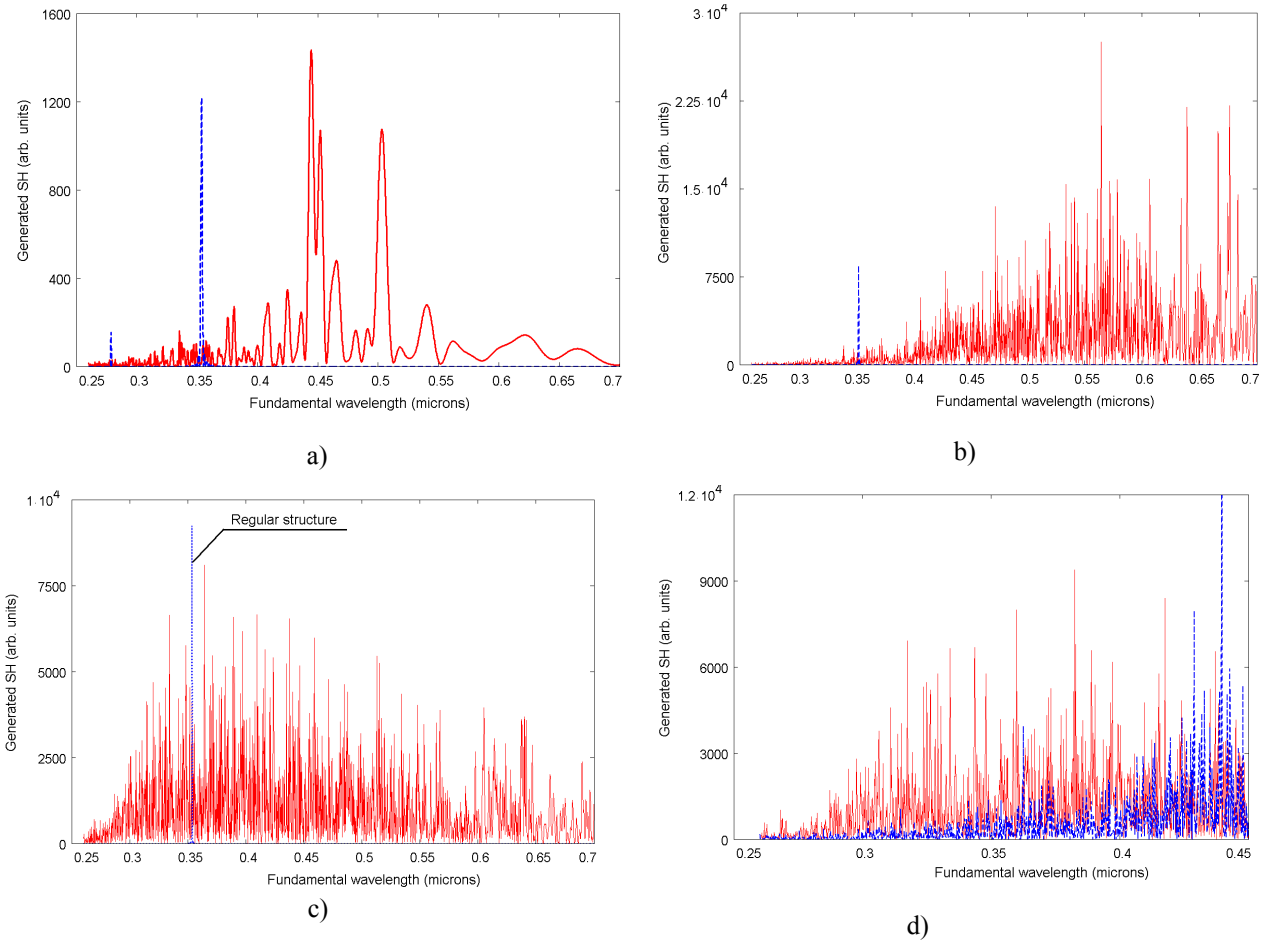

Figure 3. Calculated spectral dependences of second harmonic in a part of Sample 2 (a), the whole Sample 2 (b), and the Sample 7 (c). Dashed lines in a), b) and c) are dependencies for ideal QPM structures with the corresponding thickness (divided by 10 in Fig.2a, by 10 in Fig,2b and by 250 in Fig.2c). Comparison of short-wavelength part of these dependencies in Samples 2(dashed) and 7(solid) (d).

These two plots demonstrate that in the part of the Sample 2 with relatively weak randomization broad peaks of second harmonic are expected at fundamental wavelengths down to 0.35 – 0.4 μm, while in highly randomized structures separate much narrower peaks are observed through all the UV and visible. This feature is important when evaluating conversion of broadband radiations in random NPC. Fig. 3c presents the spectral dependence of the Sample 7 containing 1017 domains with overall thickness 928 μm; peak of regular structure of the same thickness is divided by 250. Evidently, this type of NPC structure as compared to the Sample 2 is featured by increase of short-wavelength wing of the spectrum with respect to the long-wavelength wing. At the same time, comparison between Samples 7 and 2 in the short-wavelength spectral region (Fig. 3d) is evidently in favor of the former, even despite the Sample 7 structure is more than two times shorter.

4. FOURTH HARMONIC GENERATION EXPERIMENTAL STUDY

The scheme of experimental installation is presented in Fig. 1. The central wavelength of fundamental radiation was tuned in a spectral range 740-930 nm. Maximum average power of fundamental radiation was up to 960 mW. Duration of pulses was in the range 40-100 fs. Fundamental radiation was focused into the 1 mm thick doubling nonlinear crystal BBO with a ten centimeter focal length lens. Generated second harmonic radiation was collimated by means of the second ten centimeter lens. Average power of the second harmonic was up to 135 mW that corresponds to conversion efficiency of 14.4 %. Radiation of the second harmonic was selected by means of Glan prism and focused by means of a five centimeter lens into the NPC sample. The second harmonic waist radius was 37 μm on the power level $1/e^2$ that

corresponds to peak power density up to 0.3 GW/cm^2. Polarization of the second harmonic coincided with crystallographic axis *c* so the maximum nonlinear coefficient d_{ccc} has been employed. The second harmonic after the NPC was suppressed with Acton 172-N bandpass filter with a maximum transmission at 173.5 nm, transmission at 200 nm being 6.5 %. Generated radiation at the frequency of the fourth harmonic was focused onto the entrance slit of convenient non-vacuum MSDD 1000 monochromator equipped with matrix photodetector Hamamatsu HLS192 for registration of spectrum. The monochromator's spectral resolution in a spectral range under study was 0.023 nm (5 cm^{-1}). On an axial exit of monochromator the photomultiplier Hamamatsu H5783-04 or Newport 918D sensor operating with Newport 1931-C power meter were mounted. Maximum average power radiation of the fourth harmonic on the central wavelength of 200 nm after the NPC Sample 2 was 1 μW, that corresponds to conversion efficiency 10^{-5}. The generated power can be increased by two orders at least if more powerful fundamental wave source could be employed, since optical breakdown threshold of NPC material at 400 nm for fs pulses must be expected far above intensity level used in our experiment. All measurements were done in air ambience. The NPC domain structure of the Sample 2 with the thickness of 2 mm along *a* crystallographic axis contained 262 domains. The NPC was placed on a monodomain substrate 3 mm thick in a direction.

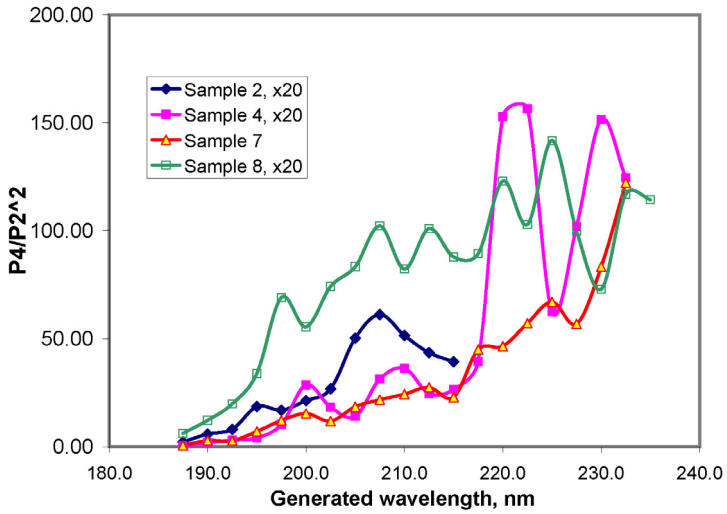

Figure 4. The fourth harmonic tuning curves in four different NPC structures of SBO.

Fig.4 presents experimental data for fourth harmonic power obtained in the four studied samples. Short wavelength decrease for all samples is due to the growing air absorption. Note that data for Samples 2, 4 and 8 are multiplied by 20. As can be expected from the calculation in Sec.3, the NPC structure in the Sample 7 is much more efficient than that in the Sample 2. The difference between similarly structured Samples 7 and 8 indicates that the latter, though being less efficient, demonstrates upraise of 200-225 nm range relatively to longer wavelengths range. At the present state of our technology we are, however, unable to connect these variations with the variations in growth conditions.

The influence of NPC structure on the spectra of the fourth harmonics is illustrated in Fig. 5, data for every sample containing four spectra obtained by tuning the fs oscillator central wavelength and BBO crystal only. Evidently, the peculiarities of spectra are not the result of random coincidence in overlapping between input radiation spectrum and the NPC band structure, but are common for all spectra for a given sample. The spectral peaks generated in the Sample 2 are the most pronounced. The Sample 4 demonstrates weaker band structure with sparsely positioned intense peaks, but the width of peaks is larger than in the Sample 2. The Samples 7 and 8 are better than the Samples 2 and 4; the fourth harmonic spectra generated in them have the less pronounced peaky structure with shallower dips, and hence, the less temporal distortion is expected. At the same time, even these samples produce radiation with spectrum far from ideal shape characteristic for angular phase matching, and further improvement of NPC technology is still desired.

The results for tuning curves and generated radiation spectra reported above are found to be applicable not for all apertures of the samples. While the Sample 2 demonstrates almost perfect homogeneity along both axes of transverse scanning, the Samples 7 and 8 produce noticeably varying harmonic signal. The results of scanning the input radiation

over the facet of these samples are presented in Fig.6. The evident inhomogeneity is understandable in view of the crystal growth model described in Sec.2 and indicates the necessity of further fine tuning the growth process for the NPC structures of this type.

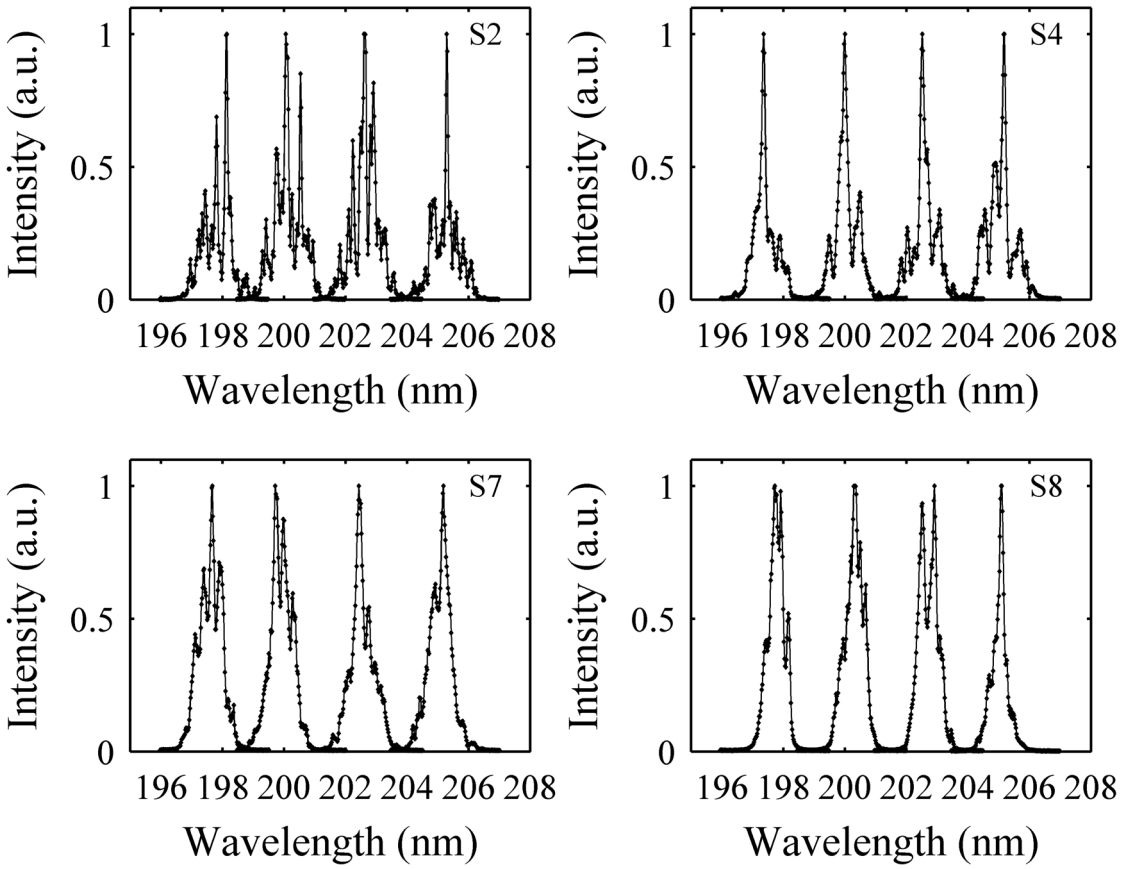

Figure 5. The spectra of the fourth harmonics of femtosecond laser generated in Samples 2, 4, 7 and 8.

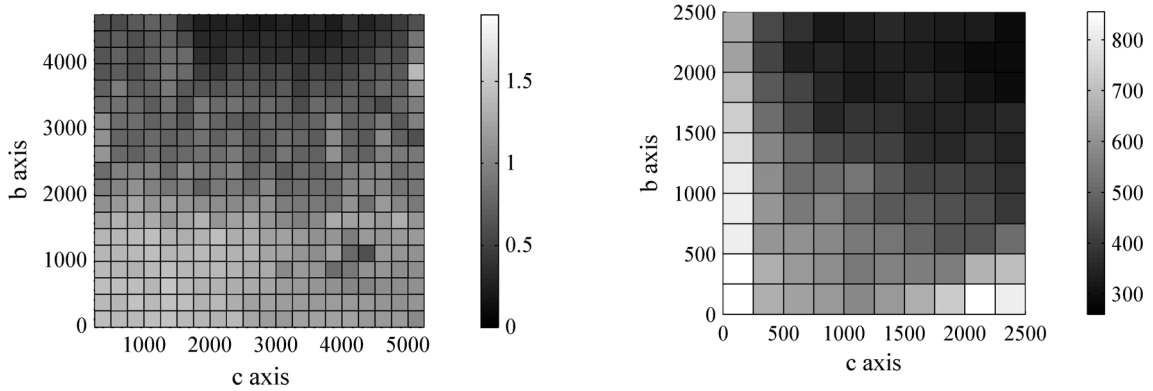

Figure 6. Transverse mapping of NPC structures via the fourth harmonic generation near 200 nm for the Sample 7 (left) and the Sample 8 (right).

5. AUTOCORRELATION MEASUREMENTS

Transparency window of SBO makes it attractive medium for diagnostics of fs pulses in the VUV. Earlier we demonstrated this possibility for NPC SBO using nonlinear diffraction from virtual beam (NLDVB)[11]. In the present study we investigate the autocorrelation measurements using RQPM. The optical scheme is the standard one with the variable delay line enabling overlapping of two crossing beams inside the NPC Sample 2. The bisector of the crossing beams, in difference with NLDVB, coincides with the *a* axis direction. Every single beam produces collinear RQPM enhanced second harmonic signal, the value of which is independent on the delay. This is the possible cause of increased background for the case of RQPM autocorrelation measurement. Tuning the delay time to the value ensuring overlapping leads to appearance of noncollinear second harmonic signal directed in the bisector direction. Fig.7 presents autocorrelation functions measured with NPC SBO and with the 500 μm thick reference BBO crystal at 800 nm central wavelength of the oscillator. Measured pulse duration was correspondingly 100 and 97 fs. Absence of chirp is evidenced by this figure (left). Main advantageous feature of RQPM in NPC SBO is its non-critical behavior in a broad spectral range of central wavelengths covering all the tuning range of our fs oscillator, with no any tuning of NPC. This is illustrated by the plot of measured pulse durations in Fig.8a. The autocorrelation signal dependence plotted in Fig. 8b reflects the RSV spectrum distribution in the NPC sample used.

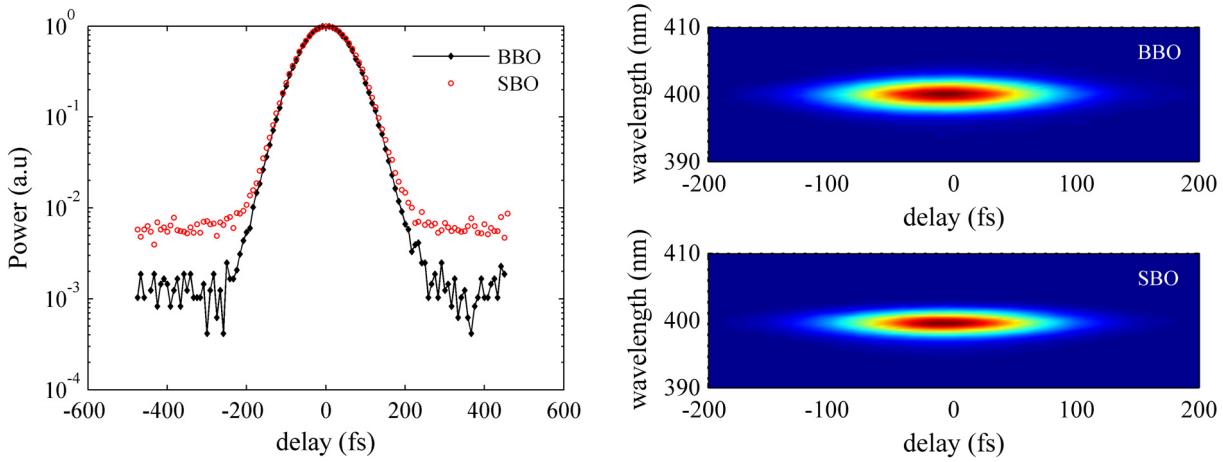

Figure 7. Autocorrelation traces and autocorrelation signal spectra for NPC SBO and BBO.

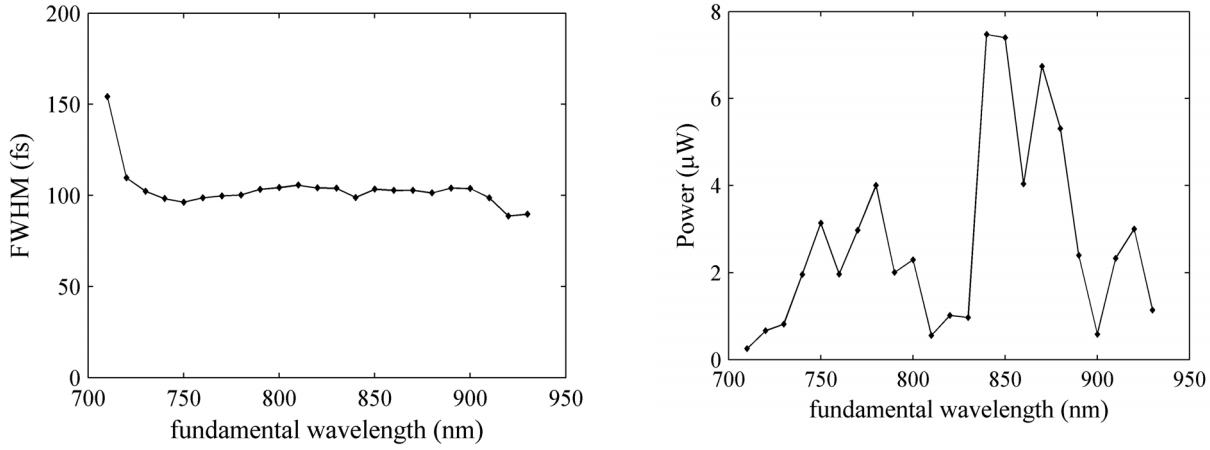

a)

Figure 8. a) Pulse durations measured with NPC SBO in RQPM geometry. b) Autocorrelation signal power dependence for NPC SBO.

6. CONCLUSION

In conclusion, typical domain structures obtainable in NPC SBO are analyzed, and their spectral properties are calculated. Tunable generation of fourth harmonic radiation of femtosecond laser of Ti: Sapphire via RQPM in NPC of SBO in spectral range from 235 to 187.5 nm was compared in different types of NPC. Behavior of the tuning curve and of the generated radiation spectra are shown to be controllable by the NPC crystal growth. The autocorrelation and pulse duration measurement of fs pulses using NPC SBO in the RQPM geometry is demonstrated, with the possibility to measure pulses in the broad spectral range with no any tuning of the nonlinear medium. The possible applications of NPC SBO are DUV and VUV converters and ultrafast diagnostics in the VUV. An interesting application would be also the generation of ultrabroad entangled photon states continuum[12] pumped with short-wavelength source.

7. ACKNOWLEDGEMENT

The work was supported by Ministry of Education and Science of Russian Federation (Contract 16.740.11.0150), Grant of President of Russian Federation for support of leading scientific schools No. SS-4645.2010.2, Grant No. RNP.2.1.1.3455, Projects 2.5.2 and 3.9.1 of PSB RAS, and Projects No. 27.1 and No. 5 of SB RAS. A.M.Vyunishev is grateful for support from RFBR (Grant 11-02-09228), from Carl Zeiss Grant and from Krasnoyarsk Regional Fund of Science and Technical Activity Support.

REFERENCES

[1] Lingli Wang, Yuhua Wang, Dan Wang, Jiachi Zhang, "Electronic structure calculations of SrB_4O_7 and SrB_4O_7:Eu crystals", Solid State Commun., 148, 331- 335 (2008).

[2] Petrov, V., Noack, F., Dezhong Shen, Feng Pan, Guangqui Shen, Xiaoqing Wang, Komatsu, R. and Alex, V., "Application of the nonlinear crystal SrB_4O_7 for ultrafast diagnostics converting to wavelengths as short as 125 nm", Opt. Lett., 29, 373 - 375 (2004).

[3] Zaitsev, A. I., Aleksandrovsky, A. S., Vasiliev, A. D., and Zamkov A. V., "Domain structure in strontium tetraborate single crystal", Journal of Crystal Growth, 310, 1 – 4 (2008).

[4] Berger, V., "Nonlinear photonic crystal", Phys. Rev. Lett., 81, 4136 - 4139 (1998).

[5] Aleksandrovsky, A. S., Vyunishev, A. M., Slabko, V. V., Zaitsev, A. I., and Zamkov, A. V., "Tunable femtosecond frequency doubling in random domain structure of strontium tetraborate", Opt. Commun. **282**, 2263 - 2266 (2009).

[6] V'yunyshev, A.M., Aleksandrovskii, A.S., Cherepakhin A.V., Rovskii, V.E., Zaitsev, A.I., Zamkov, A.V., "Frequency Doubling of Ultrashort Pulses in a Nonlinear Photonic Strontium Tetraborate Crystal", Bulletin of the Lebedev Physics Institute, **37,** 85-86 (2010).

[7] Baudrier-Raybaut, M., Haidar, R., Kupecek, Ph., Lemasson, Ph., and Rosencher, E., "Random quasi-phase-matching in bulk polycrystalline isotropic nonlinear materials", Nature, 432, 374 - 376 (2004).

[8] Fejer, M. M., Magel, G. A., Jundt, D. H. and Byer, R. L., "Quasi-phase-matched second harmonic generation: tuning and tolerances", IEEE J. Quant. Electron, 28, 2631 (1992).

[9] Aleksandrovsky, A. S., Vyunishev, A. M., Shakhura, I. E., Zaitsev, A. I, and Zamkov, A. V., "Random quasi-phase-matching in nonlinear photonic crystal structure of strontium tetraborate", Phys. Rev. A, 78, 031802(R) (2008).

[10] Aleksandrovsky, A. S., Vyunishev, A. M., Zaitsev, A. I., Zamkov, A. V., and Arkhipkin, V. G., "Detection of randomized nonlinear photonic crystal structure in a non-ferroelectric crystal", J. Opt. A, Pure Appl. Opt. **9**, S334-S338 (2007).

[11] Aleksandrovsky, A. S., Vyunishev, A. M., Zaitsev, A. I., Ikonnikov, A. A., Pospelov, G. I., "Ultrashort pulses characterization by nonlinear diffraction from virtual beam", Appl. Phys. Lett., 98, 061104 (2011).

[12] Svozilik, J., Perina, J., "Intense ultra-broadband down-conversion from randomly poled nonlinear crystals", Opt. Express, 18, 27130 (2010).